Protein states and proteinquakes

(equilibrium fluctuations/functionally important motions/hierarchy of states/glass-like structure)

ANJUM ANSARI, JOEL BERENDZEN, SAMUEL F. BOWNE†, HANS FRAUENFELDER‡, ICKO E. T. IBEN,
TODD B. SAUKE, ERRAMILLI SHYAMSUNDER, AND ROBERT D. YOUNG

Department of Physics, University of Illinois at Urbana-Champaign, 1110 West Green Street, Urbana, IL 61801

Contributed by Hans Frauenfelder, April 4, 1985

ABSTRACT   After photodissociation of carbon monoxide bound to myoglobin, the protein relaxes to the deoxy equilibrium structure in a quake-like motion. Investigation of the proteinquake and of related intramolecular equilibrium motions shows that states and motions have a hierarchical glass-like structure.

The dynamic aspects of proteins have been studied extensively in recent years and a picture of ever increasing complexity has emerged. To bring some order into the complexity, we have introduced a model that classifies states and motions (1). In the present paper, we describe the model and its experimental basis in more detail.

STATES, SUBSTATES, AND MOTIONS

We consider myoglobin (Mb), an oxygen storage protein, consisting of 153 amino acids, with molecular weight of 17,900 and approximate dimensions of $2.5 \times 4.4 \times 4.4$ nm (2). Embedded in the protein matrix is a heme group with a central iron atom, which binds small ligands such as dioxygen (O_2) or carbon monoxide (CO) reversibly. Thus, two states are involved in the function of Mb, deoxyMb and liganded Mb (e.g., MbCO). In the liganded state, the heme is planar and the iron has spin 0 and lies close to the mean heme plane. In the unliganded state, the heme group is domed, the iron has spin 2 and lies ≈ 0.5 Å away from the mean heme plane, and the globin structure differs somewhat from the liganded one (3).

A protein molecule in a particular state can assume a very large number of conformational substates (CS) (4–6). Different substates have the same overall structure, but they differ in details; they perform the same function, but with different rates.

The existence of states and of substates implies two types of motions in proteins—equilibrium fluctuations (EF) and functionally important motions (FIMs). In EF, a resting protein moves from one substate to another; the fluctuations in internal energy and entropy are determined by equilibrium thermodynamics (7). FIMs are nonequilibrium processes that lead from one state to another. If the initial and final state in a FIM are close in structure, we can assume that similar substates are involved in the EF and the FIM. The rates of the EF and the FIM are then related by fluctuation–dissipation theorems (8, 9). EF can be studied on resting proteins but FIMs require observation of a protein reaction. A protein reaction is similar to an earthquake: A stress is relieved at the focus. The released strain energy is dissipated in the form of waves and through the propagation of a deformation. The situation in Mb is shown in Fig. 1. On binding, the protein is stressed, on photodissociation, the stress is relieved. In either case, the protein finds itself in a state far from
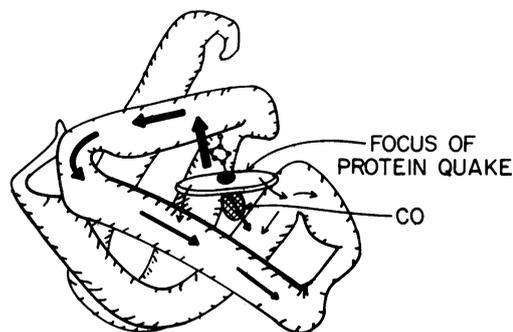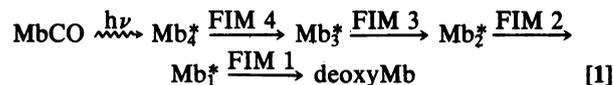
FIG. 1.   Proteinquake. Binding or dissociation of a ligand at the heme iron causes a proteinquake.

equilibrium (10). Return to equilibrium occurs through a proteinquake: the released strain energy is dissipated through waves [phonons (11) or solitons (12)] and through the propagation of a deformation (2, 3).

HIERARCHY OF SUBSTATES

The experiments described in the next section imply that the proteinquake released by photodissociation of MbCO propagates sequentially:

$$MbCO \xrightarrow{h\nu} Mb_4^* \xrightarrow{FIM\ 4} Mb_3^* \xrightarrow{FIM\ 3} Mb_2^* \xrightarrow{FIM\ 2}$$
$$Mb_1^* \xrightarrow{FIM\ 1} deoxyMb \qquad [1]$$

Mb_4^*–Mb_1^* are intermediate protein states. FIM 4 occurs rapidly even at 3 K, FIM 3 takes place near 20 K, FIM 2 starts at ≈ 40 K, and FIM 1 sets in at ≈ 210 K: As the proteinquake progresses, substates separated by larger and larger barriers become involved.

X-ray diffraction data show that the difference in structure between MbCO and deoxyMb is observable, but small (2, 3). We therefore assume that the same substates participate both in fluctuations and in dissipative motions. The existence of four FIMs then implies the existence of four tiers of substates, CS^4–CS^1. The arrangement of protein substates, shown schematically in Fig. 2, consequently is much more complex than we originally anticipated (4).

The valley in the top diagram of Fig. 2a represents one state, say MbCO. MbCO can exist in a large number of conformational substates, CS^1, separated by high barriers. Each valley in the first tier is structured into substates (CS^2) with smaller barriers. The furcation continues through two more tiers, with decreasing barrier heights. The dynamic

Biophysics: Ansari *et al.*
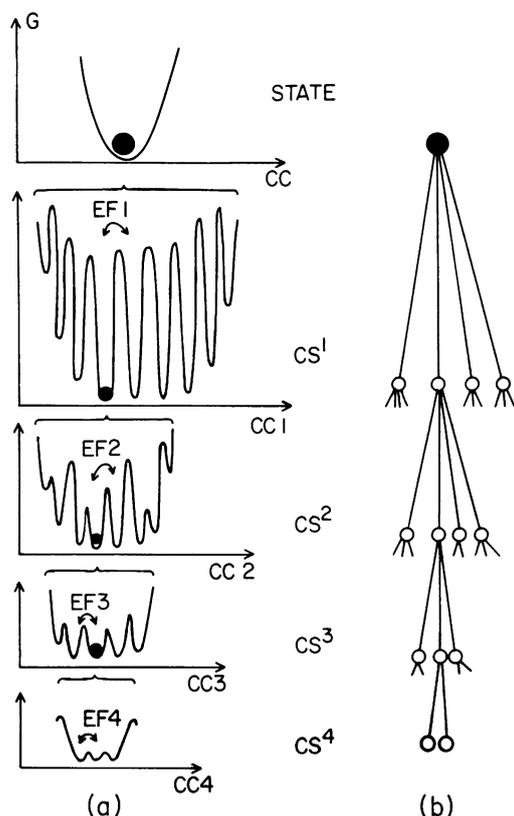
Proc. Natl. Acad. Sci. USA 82 (1985) 5001

FIG. 2. Hierarchical arrangement of the CS in myoglobin. (*a*) Schematic energy surfaces. (*b*) Tree diagram. G, Gibbs energy of the protein; CC (1–4) a conformation coordinate of tiers 1–4.

behavior of the system depends on temperature. Below ≈20 K, only fluctuations among the CS^4 occur. Above ≈20 K, the EF4 are so fast that the CS^4 within a given valley of the third tier are in thermal equilibrium. Fluctuations among the CS^3 now set in, with rates increasing with temperature. At 200 K, the structure of the second tier begins to average out, but fluctuations among the substates of the first tier set in.

EXPERIMENTAL JUSTIFICATION

The decisive experiment that leads to the hierarchical model of Fig. 2 is the observation of the relaxation of MbCO after photodissociation at temperatures between 40 and 160 K (1, 13). The experiment is sketched below. Here we do not repeat the path by which we initially arrived at the hierarchical model, but we follow the proteinquake induced by a laser flash in MbCO, starting at low temperatures and/or short times. This approach leads to the recognition of four tiers of substates. For each tier, we also cite information from experiments on resting proteins.

In flash photolysis, MbCO is placed in a cryostat, the bond between the heme iron and the CO is broken by a laser flash, and the subsequent phenomena are monitored in the visible (4) and in the near infrared (1, 13), or through Raman scattering (14). In photodissociation, the iron changes spin and the Fe-CO bond is broken within <250 fsec (15). As indicated in Eq. 1, the heme group and the protein are in the nonequilibrium state Mb_4^*, and two processes start: The quake begins as the protein relaxes toward the new equilibrium state deoxyMb. In competition with the relaxation, CO rebinds and the protein returns to the MbCO state. We do not consider the rebinding process and it is not shown in Eq. 1. The interpretation of the experiments is aided by the calculations of Karplus and collaborators (16). Their work predicts that the allosteric core, composed of the heme, histidine F8,

the FG corner, and part of the F helix, plays a crucial role in the protein relaxation.

Tier 4. Relaxation starts at the focus of the quake, the heme iron. After photodissociation at 300 K, a deoxy-like optical spectrum appears after 350 fsec (15) and the iron–histidine stretching mode reaches the deoxy value within 30 psec (17). At 3 K, we have observed deoxy-like spectra at 1 μsec after photodissociation. These values imply an apparent activation energy of <0.4 kJ/mol for $Mb_4^* \xrightarrow{\text{FIM 4}} Mb_3^*$ and the possibility of tunneling. Independent evidence for tier 4 and CS^4 comes from the specific heat of metmyoglobin crystals below 1 K (18, 19). The temperature dependence is similar to that of glasses and suggests a few tunnel states per molecule. The heights of the barriers separating these substates must be of the order of 1 kJ/mol, consistent with the estimate of ≤0.4 kJ/mol for FIM 4.

We interpret FIM 4 as partial motion of the iron out of the heme plane. The short time required for FIM 4 agrees with calculations of Henry *et al.* (20). The character of Mb_3^* is elucidated by CW resonance Raman experiments of Rousseau and Argade who find a deoxy-like spectrum of photodissociated Mb at 4.2 K and below, but with a heme core larger than deoxyMb. They suggest that the unrelaxed globin prevents the iron from moving fully out of the heme plane.

Tier 3. Evidence for the second phase of the proteinquake, $Mb_3^* \xrightarrow{\text{FIM 3}} Mb_2^*$, comes from Raman experiments. The CW Raman spectra suggest that the enlarged heme core has relaxed to its deoxy size at 20 K. At 300 K, the Raman spectrum is unrelaxed at 25 psec (22), but it is relaxed at 10 nsec. These data indicate an activation energy for FIM 3 between 1 and 5 kJ/mol. Barrier values of the order of a few kJ/mol have been found in microwave absorption experiments on hemoglobin (23) and it is possible that these correspond to the EF3. We tentatively interpret Mb_3^* as the state where the iron has moved out of the heme plane, the heme is domed, but the globin has not yet relaxed.

Tier 2. At temperature below ≈30 K, the state Mb_2^* is metastable. Mb_2^* differs from deoxyMb (24–28). Yonetani and co-workers (24) noticed that the deoxyMb line near 758 nm (band III) is red-shifted by ≈10 nm after photodissociation at 4.2 K. Band III is sensitive to the local conformation near the heme iron because it is a charge-transfer transition involving iron and porphyrin states (29, 30). We use this sensitivity to investigate FIM 2 ($Mb_2^* \rightarrow Mb_1^*$) by determining the position of the peak of band III at various temperatures as a function of the time t after photodissociation (13). The extinction coefficient of band III is small ($150 \text{ M}^{-1}\cdot\text{cm}^{-1}$). To obtain adequate signals, we use a cell 1 mm deep and 10 mm wide. MbCO (1 mM) in the cell is photodissociated with a 20 nsec, 530 nm, 0.3 J laser pulse passing through the 1-mm depth. Band III is monitored with light from diodes (Hitachi HLP40RB) mounted on the narrow side of the cell. The light traverses the 10-mm width of the cell, passes through a monochromator, and is detected with a R955 Hamamatsu photomultiplier. Fig. 3 gives band III at 80 K at various times after photodissociation.

The shift of band III after photodissociation shows two unexpected features: (*i*) No isosbestic point exists; the band shifts without appreciably broadening. The absence of an isosbestic point implies that $Mb_2^* \rightarrow Mb_1^*$ is not a two-state transition. The pathway must be complex, as sketched in Fig. 4, where the Gibbs energy of the protein is plotted as a function of a one-dimensional conformational coordinate. (*ii*) As demonstrated in Fig. 5, the shift of the peak wavenumber $\nu_p(t)$ is not exponential in time. We characterize the extent of relaxation by the fractional displacement of $\nu_p(t)$ from the measured static deoxy peak value, $\nu_p(\infty)$: $\delta(t) = [\nu_p(t) - \nu_p(\infty)]/[\nu_p(0) - \nu_p(\infty)]$. We assume that $\nu_p(0) - \nu_p(\infty)$ is independent of temperature and that the
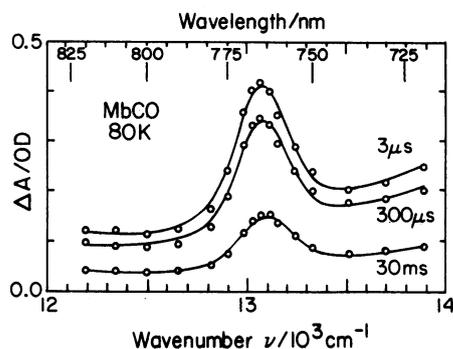
FIG. 3.   Band III as function of time after photodissociation at 80 K. The area under the peak decreases with time owing to recombination.

pathway $Mb_2^* \rightarrow Mb_1^*$, can be described by a distribution of activation energies. Denoting with $\rho(E_2)dE_2$ the probability of finding a barrier with activation energy between E_2 and $E_2 + dE_2$ we get

$$\delta(t) = \int dE_2 \, \rho(E_2) \exp(-k_2 t). \qquad [2]$$

We fit the data with $k_2 = A_2 \exp(-E_2/RT)$ and a box distribution,

$$\rho(E_2) = \begin{cases} (E_{max} - E_{min})^{-1}, & E_{min} \le E_2 \le E_{max} . \\ 0 & , \text{otherwise} \end{cases} \qquad [3]$$

The solid lines in Fig. 5 are fits with $A_2 = 10^{13} \ sec^{-1}$, $E_{min} = 12 \ kJ/mol$, $E_{max} = 41 \ kJ/mol$. The fit is satisfactory at all temperatures except 100 K. Fig. 6 gives the range of relaxation rates covered by FIM 2 as a function of $10^3/T$. The structural interpretation of FIM 2 is not yet clear; it may correspond to motion of the residues of the allosteric core (16) and a tilting of the proximal histidine (2, 3, 31).

The activation energy distribution of FIM 2 suggests, through the relation between fluctuations and dissipation, activation energies between 10 and 40 kJ/mol for the fluctuations in the second tier (EF2). Support for such EF in heme proteins comes from experiments such as Mössbauer effect (1, 32–34), fluorescence quenching (35, 36), fluorescence line narrowing (T. W. Scott and J. M. Friedman, personal communication), and NMR (38).

Tier 1. The existence of tier 1 substates (CS^1) follows from a comparison of FIM 2 (Fig. 6) with CO binding data (4). The nonexponential time dependence of CO binding to Mb at temperatures below ≈200 K initially motivated the introduction of substates (4, 5). At 160 K, for instance, CO binding follows a power law to at least 0.1 sec; thus transitions among the substates responsible for the nonexponential binding must be slower than 0.1 sec. Fig. 6 shows, however, that most of FIM 2 is faster than 0.1 sec at 160 K. The substates of tier
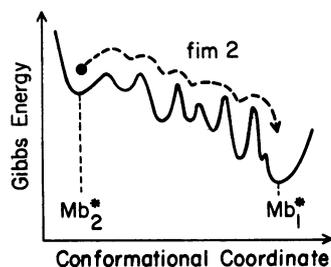

FIG. 4.   Schematic representation of the Gibbs energy of myoglobin as function of a conformational coordinate.
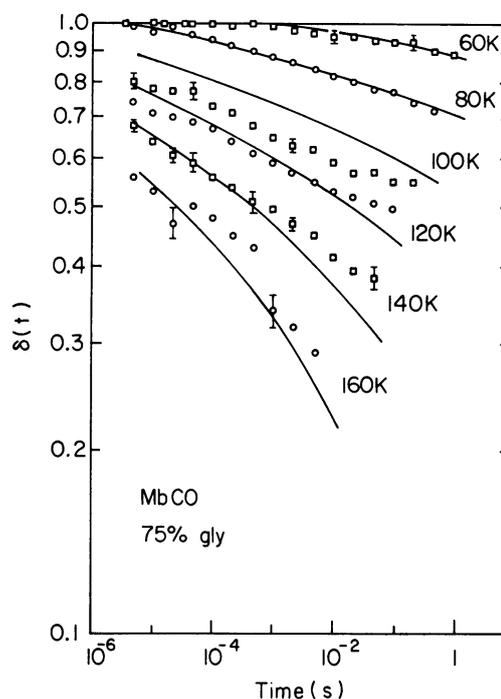

FIG. 5.   Fractional displacement of peak position ν_p of band III from equilibrium deoxy value, $\delta(t) = [\nu_p(t) - \nu_p(\infty)]/[\nu_p(0) - \nu_p(\infty)]$ as function of time after photodissociation at various temperatures. The solid lines are fits to the data using Eq. **2**.

2 cannot be responsible for the nonexponential binding; another tier must exist. This conclusion is supported by a pressure titration experiment, which proves that relaxation of the substates within 100 sec is absent at 200 K, but complete at 220 K (39). The narrow temperature interval over which EF1 sets in suggests a glass-like phase transformation. The structural features involved in FIM 1 are not yet known, but it is likely that a major part of the protein, including the hydration shell, participates.

Further evidence for the existence of CS^1 comes from comparing experiments that probe motions near the heme iron with those that either explore the entire protein or look at the protein surface. The mean-square displacement for metMb as determined by Mössbauer effect (33), $\langle x^2 \rangle_{Mb}$, is sensitive to the motion of the iron and hence to EF2. In
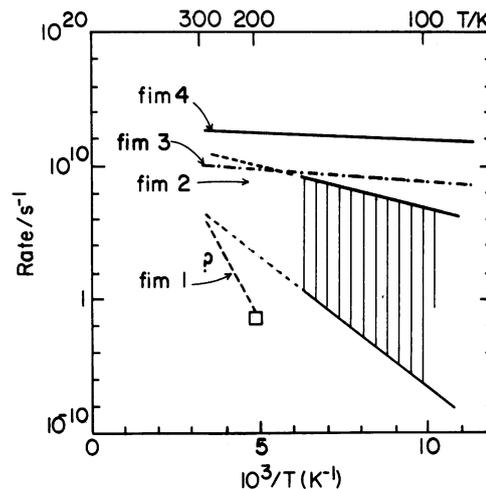

FIG. 6.   Relaxation rates for FIMs 1 to 4 as function of $10^3/T$. For FIM 2, the ranges of rates are indicated.

Biophysics: Ansari *et al.*

Proc. Natl. Acad. Sci. USA 82 (1985) 5003

contrast, the mean-square displacement for Rayleigh scattering (40), $\langle x^2 \rangle_R$, gives an average over the entire protein and should have contributions from EF2 and EF1. $\langle x^2 \rangle_{M\ddot{o}}$ and $\langle x^2 \rangle_R$ have the same temperature dependence up to $\approx$260 K. Above 260 K, $\langle x^2 \rangle_R$ increases much more rapidly with temperature, as is expected for EF1. By using a two-state model, the temperature dependence of $\langle x^2 \rangle_R - \langle x^2 \rangle_{M\ddot{o}}$ can be fit with a rate $k_1 = A_1 \exp(-E_1/RT)$, $A_1 \approx 10^{20}$ sec^{-1}, $E_1 \approx 70$ kJ/mol. A_1 and $E1$ are similar to estimates obtained earlier (4). Additional evidence for the existence of CS^1 and CS^2 comes from a comparison of the relaxation rate k_M for the Mössbauer effect (41) with the rate k_ϵ for microwave absorption in the hydration shell (42): k_M and k_ϵ differ markedly in activation energy and preexponential. In agreement with FIM 2 (Fig. 6), k_M is of the order of 10^8 sec^{-1} even at 180 K, while k_ϵ drops essentially to zero at $\approx$210 K, where EF1 also ceases.

SUMMARY, CONNECTIONS, AND PROBLEMS

The Hierarchical Protein Model. The principal results of the present paper are as follows: (*i*) A globular protein can exist in a large number of conformational substates separated by barriers, some of which become effectively infinitely high below $\approx$210 K (CS^1). (*ii*) Transitions among substates are EF; nonequilibrium transitions from one protein state to another involve FIMs. (*iii*) Substates and equilibrium fluctuations possess hierarchies as shown in Fig. 2. In myoglobin, four different tiers of substates and motions are observed. (*iv*) A transition from one protein state to another can involve a proteinquake. Strain energy is released and propagates through the protein, in an interplay of EF and FIMs (Fig. 7). (*v*) The relaxation process FIM 2 (Figs. 3 and 5) is not exponential in time and cannot be described by a two-state transition. (*vi*) The distributions in relaxation rates (Eq. 3) and in the activation enthalpies for CO binding (4) imply that different substates possess properties that must be described by distributions.

Proteinquakes. In a generalization of Fig. 5, the proteinquake (Eq. 1) can be represented as in Fig. 7. Consider first temperatures below 5 K. Before photodissociation, a particular MbCO protein will be in a certain CS^3 undergoing EF4 among the various CS^4 (Fig. 2). On photodissociation, a new equilibrium potential surface is established as indicated in Fig. 7. The protein represented by the bullet makes the transition MbCO $\xrightarrow{h\nu}$ Mb$_4^*$ $\xrightarrow{\text{FIM 4}}$ Mb$_3^*$, gets stuck in Mb$_3^*$, and fluctuates there. As the temperature is increased, the protein can move more and more. Finally, above $\approx$210 K, relaxation is completed through FIM 1, and the protein is in the deoxy state and fluctuates (EF1) among the substates
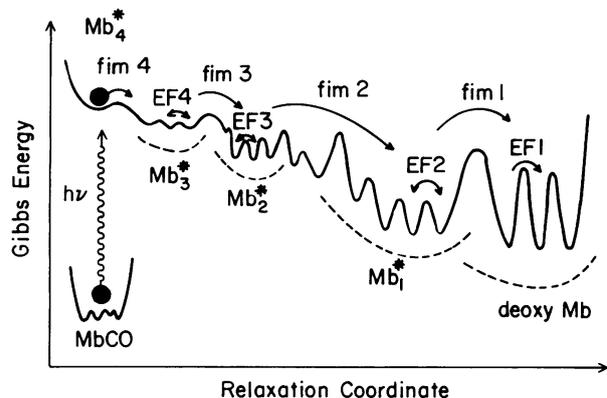
CS^1. While Fig. 7 appears complicated, the true complexity is still hidden. The number of initial and intermediate states is very large and Fig. 7 shows only one pathway. The actual quake is an average over all possible pathways.

Are Proteins and Glasses Related? The nonexponential time dependence of ligand binding and the low-temperature specific heat data have led to the suggestion that proteins are similar to glasses (18, 19, 43). The present work implies that the analogy is apt. The characteristics of glasses and spin glasses (44, 45) have correspondences in proteins. The static properties match: below a critical temperature ($\approx$210 K in myoglobin), there exists a large number of energy valleys separated by effectively infinitely high barriers, the system is nonergodic (46), and properties vary from valley to valley (substate to substate). The substates possess a hierarchical structure, the tree diagram in Fig. 2b resembles the tree of Parisi, and the protein substate structure may be ultrametric (44, 45). The dynamic properties remain to be explored in more depth but what is known reinforces the relationship between proteins and glasses: Relaxation (the proteinquake) is sequential and nonexponential in time, as suggested for glasses (47, 48). Glass theories may apply to proteins and proteins may test glass theories.

Problems. Experimentally and theoretically, much remains to be done. We have barely begun to look at the various tiers of substates and motions, and we have not yet studied their dependence on protein structure and external parameters. We do not know if more than four tiers of substates exist or if substates fall into discrete classes, as suggested here, or if they form a continuum. The connection between equilibrium fluctuations and nonequilibrium motions has only been considered in a superficial way (1). Is the description (Eq. 2) of the nonexponential time dependence of FIM 2 in terms of an activation energy spectrum valid? Are the motions hierarchical so that, for instance, FIM 2 can only proceed after FIM 3 (47)? Which of the FIMs are truly important for the function and how? Similarities and differences between proteins and glasses remain to be explored. Connections of the hierarchical model introduced here to other treatments (e.g., see refs. 49–52) should be considered. A possible link between the tiers of substates and the hierarchy of domains within proteins remains to be investigated (21, 37).

FIG. 7. Proteinquake, described in the hierarchical structure of Fig. 2.

1. Frauenfelder, H. (1985) in *Structure and Motion: Membranes, Nucleic Acids and Proteins*, eds. Clementi, E., Corongiu, G., Sarma, M. H. & Sarma, R. H. (Adenine, Guilderland, NY), pp. 205–218.
2. Dickerson, R. E. & Geiss, I. (1983) *Hemoglobin: Structure, Function, Evolution and Pathology* (Benjamin–Cummings, Menlo Park, CA).
3. Phillips, S. E. V. (1980) *J. Mol. Biol.* **142**, 531–554.
4. Austin, R. H., Beeson, K. W., Eisenstein, L., Frauenfelder, H. & Gunsalus, I. C. (1975) *Biochemistry* **14**, 5355–5373.
5. Frauenfelder, H. (1983) in *Structure and Dynamics: Nucleic Acids and Proteins*, eds. Clementi, E. & Sarma, R. H. (Adenine, Guilderland, NY), pp. 369–376.
6. Frauenfelder, H., Petsko, G. A. & Tsernoglou, D. (1979) *Nature (London)* **280**, 558–563.
7. Cooper, A. (1976) *Proc. Natl. Acad. Sci. USA* **73**, 2740–2741.
8. Kubo, R. (1966) *Rep. Prog. Phys.* **29**, 255–284.
9. Suzuki, M. (1975) *Prog. Theor. Phys.* **56**, 77–94.
10. Blumenfeld, L. A. (1978) *Q. Rev. Biophys.* **11**, 251–308.

11. Chou, K. C. & Chen, N. Y. (1977) *Sci. Sin.* **20**, 447–457.
12. Davydov, A. S. (1983) in *Structure and Dynamics: Nucleic Acids and Proteins*, eds. Clementi, E. & Sarma, R. H. (Adenine, Guilderland, NY), pp. 377–387.
13. Bowne, S. F. (1984) Dissertation (University of Illinois, Urbana–Champaign).
14. Friedman, J. M., Rousseau, D. L. & Ondrias, M. R. (1982) *Annu. Rev. Phys. Chem.* **33**, 471–491.
15. Martin, J. L., Migus, A., Poyart, C., Lecarpentier, Y., Astier, R. & Antonetti, A. (1983) *Proc. Natl. Acad. Sci. USA* **80**, 173–177.
16. Gelin, B. R., Lee, A. W.-M. & Karplus, M. (1983) *J. Mol. Biol.* **171**, 489–559.
17. Findsen, E. W., Scott, T. W., Friedman, J. M., Ondrias, M. R. & Chance, M. R. (1985) *J. Am. Chem. Soc.*, in press.
18. Goldanskii, V. I., Krupyanskii, Yu. F. & Fleurov, V. N. (1983) *Doklady Akad. Nauk SSSR* **272**, 978–981.
19. Singh, G. P., Schink, H. J., Lohneysen, H. v., Parak, F. & Hunklinger, S. (1984) *Z. Phys. B.* **55**, 23–26.
20. Henry, E. R., Levitt, M. & Eaton, W. A. (1985) *Proc. Natl. Acad. Sci. USA* **82**, 2034–2038.
21. Bennett, W. S. & Huber, R. (1982) *Crit. Rev. Biochem.* **15**, 291–384.
22. Johnston, C., Dalickas, G., Gupta, D., Spiro, T. & Hochstrasser, R. (1985) *Biochemistry*, in press.
23. Genzel, L., Kremer, F., Poglitsch, A. & Bechtold, G. (1983) *Biopolymers* **22**, 1715–1729.
24. Iizuka, T., Yamamoto, H., Kotani, M. & Yonetani, T. (1974) *Biochim. Biophys. Acta* **371**, 126–139.
25. Spartalian, K., Lang, G. & Yonetani, T. (1976) *Biochim. Biophys. Acta* **428**, 281–290.
26. Sharonov, Y. A., Sharonova, N. A., Figlovsky, V. A. & Grigorjev, V. (1982) *Biochim. Biophys. Acta* **709**, 332–341.
27. Ondrias, M. R., Rousseau, D. L. & Simon, S. R. (1983) *J. Biol. Chem.* **258**, 5638–5642.
28. Roder, H., Berendzen, J., Bowne, S. F., Frauenfelder, H., Sauke, T. B., Shyamsunder, E. & Weissman, M. B. (1984) *Proc. Natl. Acad. Sci. USA* **81**, 2359–2363.
29. Eaton, W. A. & Hofrichter, J. (1981) *Methods Enzymol.* **76**, 175–261.
30. Makinen, M. W. & Churg, A. K. (1983) in *Iron Porphyrin Part I*, eds. Lever, A. B. P. & Gray, H. B. (Addison-Wesley, Reading, MA), pp. 141–235.
31. Friedman, J. M., Scott, T. W., Stepnoski, R. A., Ikeda-Saito, M. & Yonetani, T. (1983) *J. Biol. Chem.* **258**, 10564–10572.
32. Keller, H. & Debrunner, P. (1980) *Phys. Rev. Lett.* **45**, 68–71.
33. Parak, F., Frolov, E. N., Mössbauer, R. L. & Goldanskii, V. I. (1981) *J. Mol. Biol.* **145**, 824–833.
34. Bauminger, E. R., Cohen, S. G., Nowik, I., Ofer, S. & Yariv, J. (1983) *Proc. Natl. Acad. Sci. USA* **80**, 736–740.
35. Lakowicz, J. R. & Weber, G. (1973) *Biochemistry* **12**, 4171–4179.
36. Eftink, M. R. & Ghiron, C. A. (1975) *Proc. Natl. Acad. Sci. USA* **72**, 3290–3294.
37. Janin, J. & Wodak, S. S. (1983) *Prog. Biophys. Mol. Biol.* **42**, 21–78.
38. Andrew, E. R., Bryant, D. J. & Cashell, E. M. (1980) *Chem. Phys. Lett.* **69**, 551–554.
39. Eisenstein, L. & Frauenfelder, H. (1978) *Frontiers of Biological Energetics* (Academic, New York), Vol. I, pp. 680–688.
40. Krupyanskii, Yu., Parak, F., Engelman, D., Mössbauer, R. L., Goldanskii, V. I. & Suszcheliev, I. (1982) *Z. Naturforsch. C.* **37**, 57–62.
41. Parak, F. (1986) *Methods Enzymol.*, in press.
42. Singh, G. P., Parak, F., Hunklinger, S. & Dransfeld, K. (1981) *Phys. Rev. Lett.* **47**, 685–688.
43. Stein, D. (1985) *Proc. Natl. Acad. Sci. USA* **82**, 3670–3672.
44. Toulouse, G. (1984) *Helv. Phys. Acta* **57**, 459–469.
45. Mézard, M., Parisi, G., Sourlas, N., Toulouse, G. & Virasoro, M. (1984) *Phys. Rev. Lett.* **52**, 1156–1159.
46. Palmer, R. G. (1982) *Adv. Phys.* **31**, 669–735.
47. Palmer, R. G., Stein, D. L., Abrahams, E. & Anderson, P. W. (1984) *Phys. Rev. Lett.* **53**, 958–961.
48. Huberman, B. A. & Kerszberg, M. (1985) *J. Phys. A*, **18**, 331–336.
49. Richards, F. M. (1979) *Carlsberg Res. Commun.* **44**, 47–63.
50. Agmon, N. & Hopfield, J. J. (1983) *J. Chem. Phys.* **79**, 2042–2053.
51. Young, R. D. & Bowne, S. F. (1984) *J. Chem. Phys.* **81**, 3730–3737.
52. Parak, F. & Knapp, E. W. (1984) *Proc. Natl. Acad. Sci. USA* **81**, 7088–7092.